CMS TN/95-120
4 September, 1995

RPC geometry and Muon Trigger acceptance

M. Konecki, J. Królikowski, I. M. Kudla
Institute of Experimental Physics, Warsaw University, Poland

G. Wrochna
CERN, Geneva, Switzerland

Abstract

RPC geometry and Muon Trigger acceptance study is presented. Influence of detector dead areas on the trigger performance is discussed. Various possible trigger algorithms are compared. Recommendations for designing RPC geometry and choosing among trigger algorithms are given.

1 RPC geometrical coverage in the barrel

The CMS Muon System [1] consists of 4 muon stations (both in the barrel and in the endcaps) arranged in such a way that every high p_t muon should cross active areas of at least 3 of them. Therefore, the RPC trigger [2] is based on a coincidence of 3 out of 4 stations. Thus, the geometrical acceptance of the trigger can be defined as a probability to cross at least 3 out of 4 RPC planes (denoted as MS1,2,3,4) placed in different muon stations. A muon with $p_t <$ 5-6 GeV cannot, however, reach outermost stations due to energy losses. In order to be able to trigger on such muons the two inner stations in the barrel are equipped with additional RPC planes, denoted as MS1' and MS2'. In this case trigger requires a coincidence of at least 3 out of 4 planes: MS1,1',2,2'.

1.1 Simulation

The trigger acceptance was studied using IRIS Explorer^{TM} [3] interfaced with GEANT based simulation program CMSIM [4]. CMS layout corresponding to the Technical Proposal design [1] was simulated (Fig. 1). Average geometry of ECAL (IEVERS=-120) and HCAL (IHVERS=-41) were used. RPC dead space along each edge was assumed to be 1.5 cm, which is rather optimistic. Later engineering study indicates that it might be as big as 3 cm.

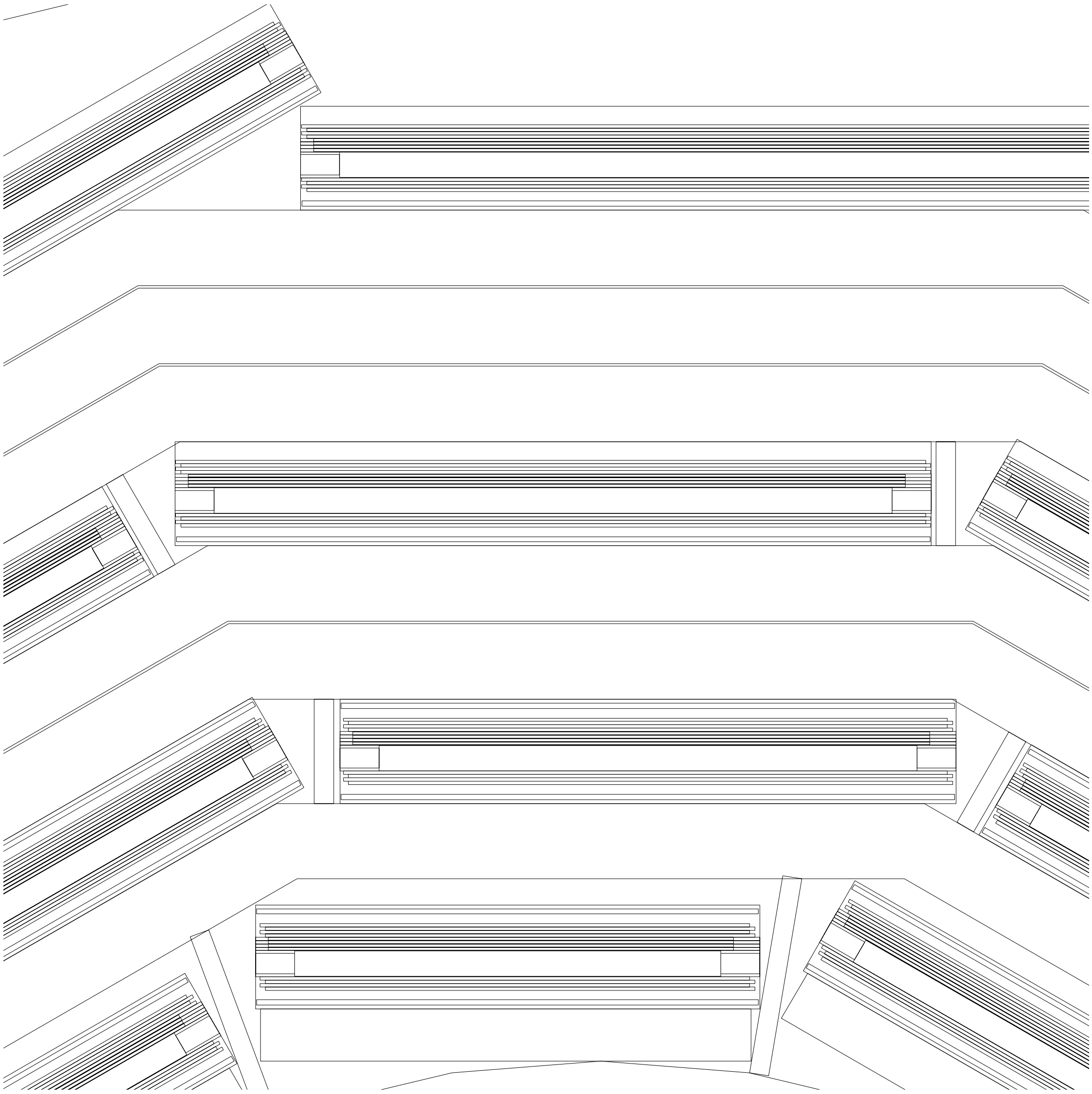

Figure 1: GEANT implementation of the muon stations layout as described in the CMS Technical Proposal.

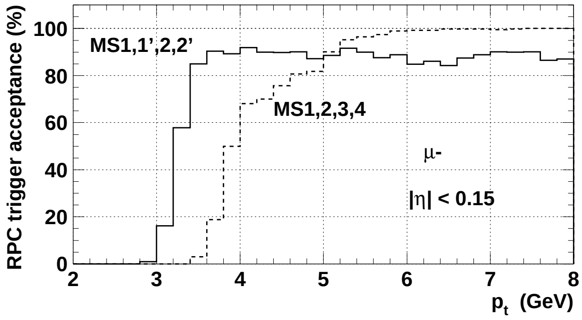

Figure 2: Geometrical acceptance of the RPC trigger defined as a probability of crossing 3 out of 4 RPC planes. At high p_t one RPC plane per station is used (solid line). At low p_t two planes of MS1 and two planes of MS2 are used (dashed line).

1.2 Acceptance losses in ϕ

1.2.1 Acceptance for high p_t muons

In order to understand the origin of possible acceptance losses we studied the ϕ and η coordinates separately. Fig. 2 shows the acceptance for $|\eta| < 0.15$, i.e. within the central wheel, where there are no gaps in η. The acceptance is integrated over all ϕ. It is seen that the high p_t algorithm based on MS1,2,3,4 is fully efficient above $p_t = 6$ GeV. Due to the staggering of the muon station a high p_t muon will always cross at least 3 of them.

1.2.2 Low p_t reach

Below 6 GeV the energy losses decrease the acceptance. Therefore, in this region the low p_t algorithm based on MS1,1',2,2' should be used. It is no more than 90% efficient because dead spaces in MS1 and 1' as well as MS2 and 2' are correlated, and, in most cases, muon crosses either 4 or 2 RPC planes. The lowest possible effective p_t cut is around 3.6 GeV. One should however keep in mind that this number is very sensitive to the amount of absorber along the muon path. The simulated geometry does not contain cables and some mechanical structures. The value of 3.6 GeV should be considered then as a lower limit rather than the most probable value. After more detailed simulation it may grow to about 4 GeV.

1.2.3 Charge asymmetry

The staggering of the muon stations slightly violates the $\pm\phi$ symmetry of the muon system. Hence, one can expect some asymmetry in the trigger acceptance for positive and negative muons. Such an asymmetry should be carefully watched because it may affect measurements of some physics quantities. Fig. 3 shows that indeed some asymmetry of the order of 4% is present around p_t = 7-8 GeV. At this moment it is difficult to judge about its possible impact on physics, because an asymmetry itself is not dangerous if it is precisely known. Therefore, one should ask not only how big the asymmetry is but also with which accuracy we know it. Anyway, the best way to reduced the asymmetry is to minimize dead areas at the corners of the stations. Some possibilities of such reduction will be discussed later.

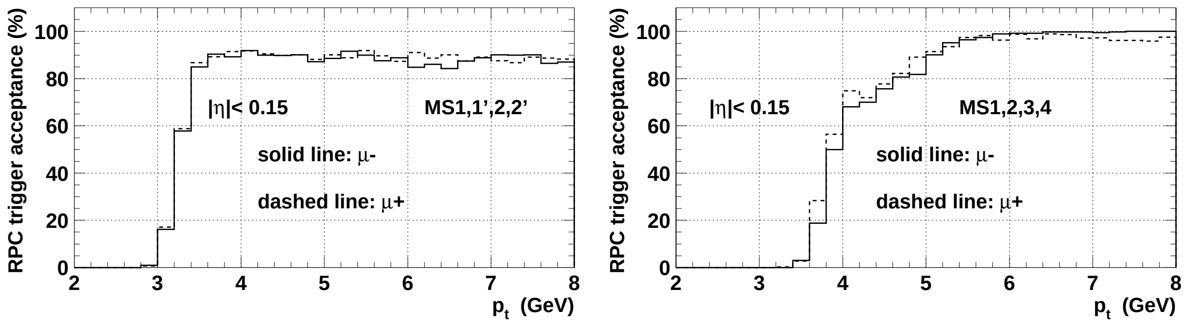

Figure 3: Charge asymmetry for low p_t (left plot) and high p_t (right plot) muons.

1.2.4 Staggering optimization

The role of staggering can be better understood by comparing the two limiting cases: maximal and minimal staggering. The maximal staggering option is the one shown in Fig. 1, which is the baseline design described in the Technical Proposal [1]. It has been simulated by the modified geometry of the CMSIM 007 program [4]. The minimal staggering was implemented in the official release of CMSIM 007 (Fig. 4). This option has smaller dead areas in each station. Therefore, the low p_t algorithm which relies on two RPC planes per station is more efficient. This can be seen in Fig. 5 (left plot). On the other hand the high p_t algorithm is not fully efficient above $p_t = 6$ GeV because the staggering is not enough to avoid overlapping of dead spaces in different stations (Fig. 5, right plot). Thus the minimal staggering is better at low p_t, whereas the maximal one performs better at high p_t. The overall conclusion is in favour of maximal staggering because the low p_t algorithm is used only upto 5-6 GeV, whereas the high p_t one covers the whole remaining region which is moreover more important from physics point of view.

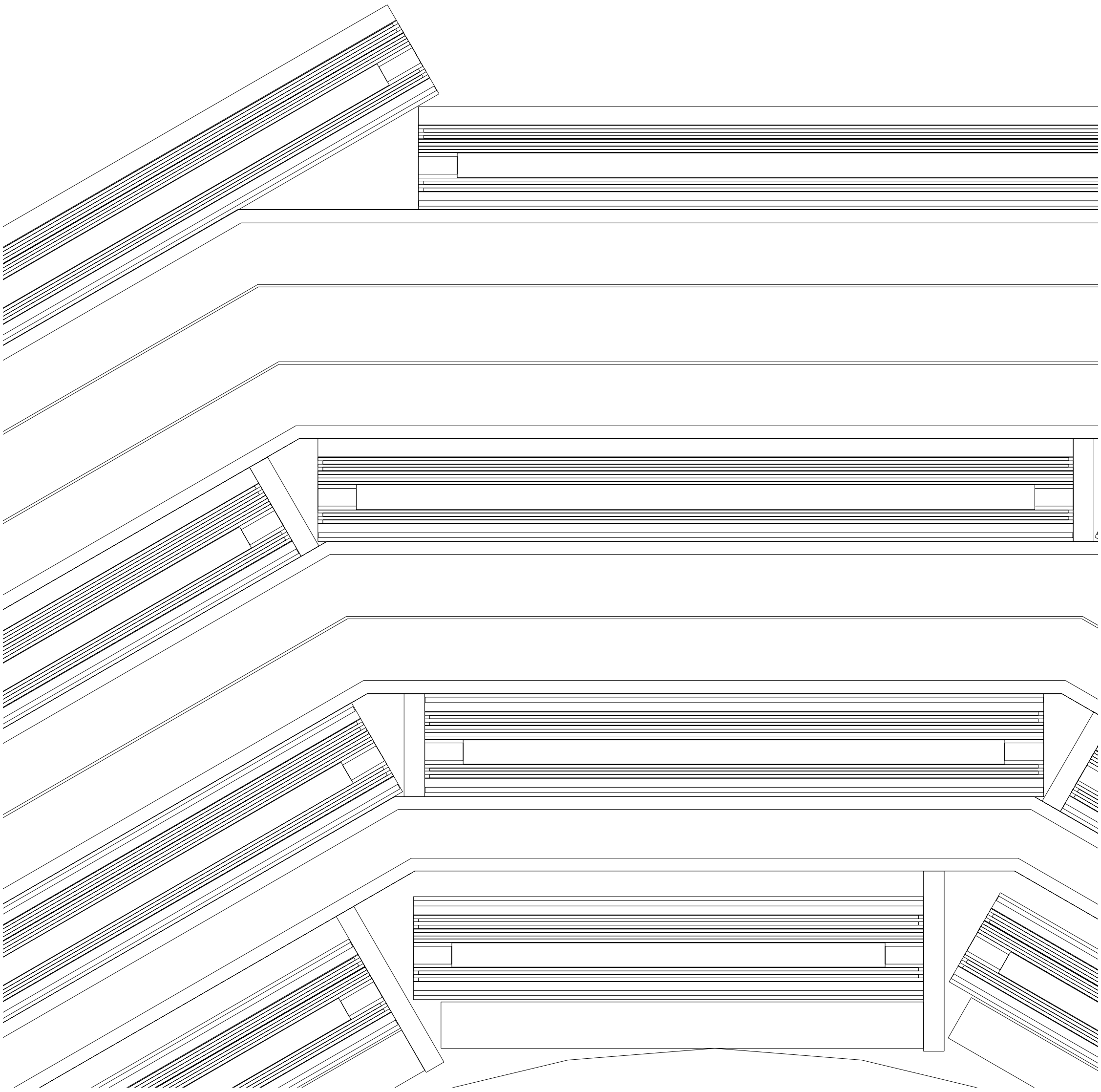

Figure 4: Layout of the muon stations implemented in CMSIM version 007. Stations are less staggered then in the CMS Technical Proposal.

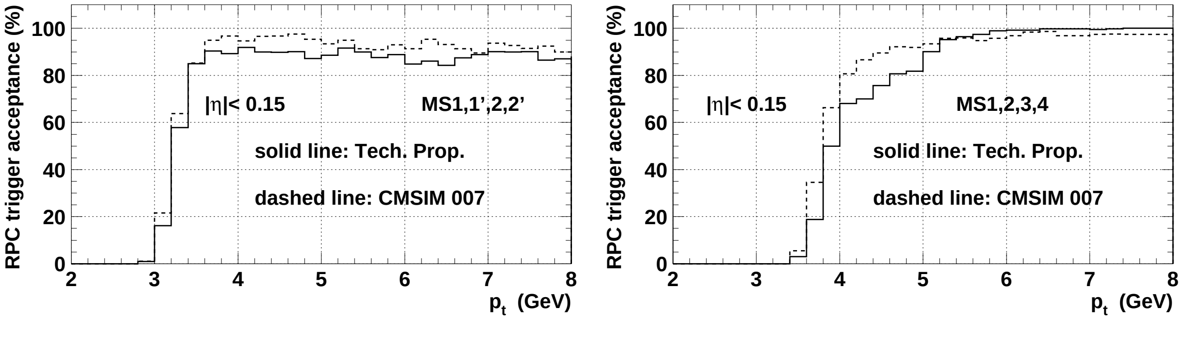

Figure 5: Comparison of maximal staggering (Technical Proposal – solid line) and minimal staggering (CMSIM 007 – dashed line) for low p_t (left plot) and high p_t (right plot) muons.

1.3 Acceptance losses in η

Possible acceptance losses in η should not depend strongly on muon p_t because the bending in the RZ plane is very small. Therefore they were studied with monoenergetic muons (1 TeV). Results are shown in Fig. 6. One can see dramatic effect of the gaps between the barrel wheels, especially for the low p_t algorithm. It is explained in Fig. 7. Muons emitted in the shadowed angles cross only two planes and have no chance to give a trigger. Therefore one should expect two completely dead areas in Fig. 6 around $\eta = 0.28$ and $\eta = 0.35$. In fact they are smeared out by the binning effect of the histogram.

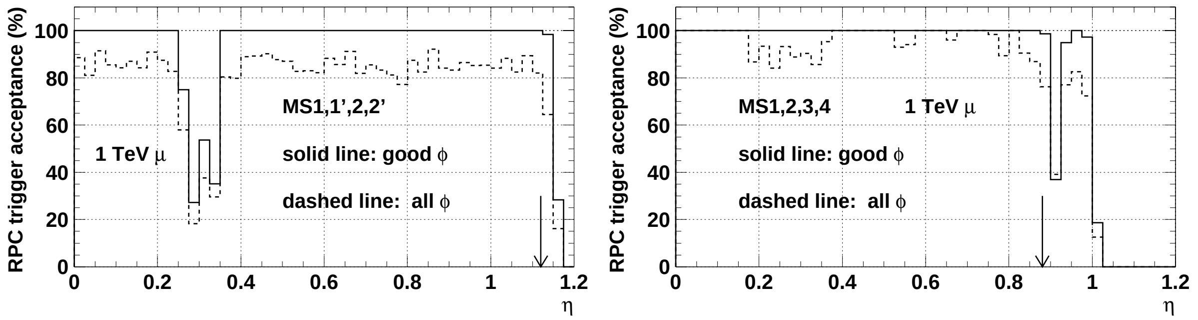

Figure 6: Rapidity dependence of the trigger acceptance in the region without ϕ gaps (solid line) and averaged over all ϕ angles (dashed line) for low p_t (left plot) and high p_t (right plot) algorithms. Arrows indicates end of the barrel where the study was performed.

There was a suggestion that extending the length of the central wheel may improve the acceptance because muons would cross the dead zones at more favourable angle. This is illustrated in Fig. 8 where the wheel length runs from 256 cm (current design – 5 equal wheels) to 426 cm (the case of 3 equal wheels). Indeed the acceptance increase with the length of the central wheel, but rather slowly. At an expense of enormous technical complications (longer wires, chamber bending under gravitation, larger tools for chamber production, etc.) one can reduce the dead zone by $\sim$ 40%. On the other hand any reduction of the gap between the wheels has an immediate positive impact on the acceptance.

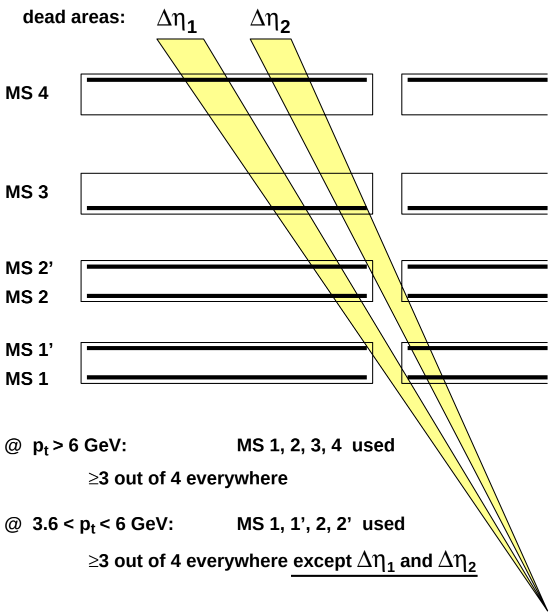

Figure 7: Origin of the trigger acceptance gap $\Delta\eta$ (< 3 RPC planes crossed by a muon). Two shadowed areas are at $\eta \approx$0.28 and 0.35.

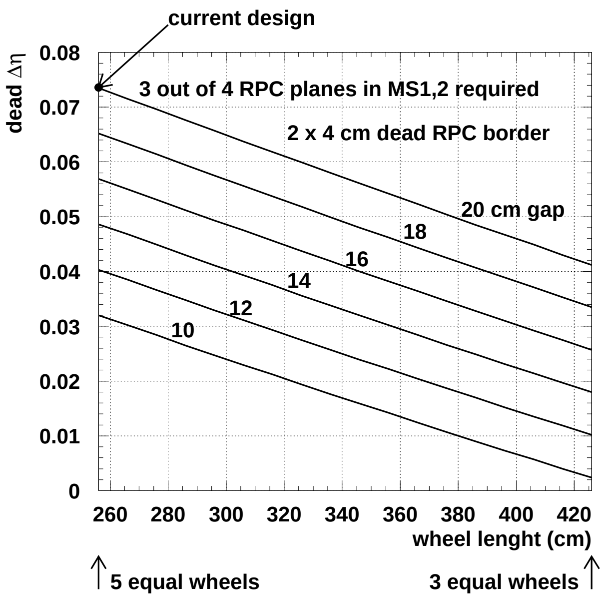

Figure 8: Size of the trigger acceptance gap $\Delta\eta$ (< 3 RPC planes crossed by a muon) for various position and width of the gap between the barrel wheels.

The acceptance loss due to the gap between the wheels in the current design is estimated to be $\approx$ 3% for the single muon and $\approx$ 6% for the double muon trigger. If we will not succeed to narrow the gap between the wheels this will remain an irreducible loss for muons with $p_t < 6$ GeV.

At high p_t (> 6 GeV) the gap do not pose a problem because, as can be seen from Fig. 6, muons always cross at least 3 out of 4 planes MS1,2,3,4.

2 Various "three out of four" algorithms

2.1 Classification of algorithms

Let us consider a muon crossing 4 triggering planes at ϕ_1, ϕ_2, ϕ_3 and ϕ_4 respectively. If it crosses active areas of the planes it create a pattern of 4 hits[1] which we denote $(\phi_1\phi_2\phi_3\phi_4)$. If one of the points (say, in the second plane) is in a dead area, only 3 hits will be created which can be denoted $(\phi_1 - \phi_3\phi_4)$. We will not consider the cases where less than 3 hits were created.

Trigger algorithms can be divided into two classes:

- **4/4 algorithms** (read: "four out of four algorithm") — only 4-fold coincidence cause a trigger
- **3/4 algorithms** — 3-fold coincidence is enough to cause a trigger; obviously 4-fold coincidence cause it as well

The 3/4 algorithms can be in turn divided into:

- **weak 3/4 algorithms** — do not distinguish 4-fold and 3-fold coincidences
- **strong 3/4 algorithms** — which may, in principle, assign different p_t to 4-fold and to 3-fold coincidences and set a so called "quality bit" in the case of 4-fold coincidence

Another possible division of 3/4 algorithms is into:

- **random 3/4 algorithms** — which do not distinguish which plane was missing and assign the same momentum for all of them
- **non-random 3/4 algorithms** — which may, in principle, assign different p_t to each of the 3/4 patterns: $(-\phi_2\phi_3\phi_4)$, $(\phi_1 - \phi_3\phi_4)$, $(\phi_1\phi_2 - \phi_4)$, $(\phi_1\phi_2\phi_3-)$.

The "random 3/4 algorithms" can be realised in practice either by "scanning" the coincidence inputs with the logical "1" or replacing the coincidence by a counter with threshold = 3 (see Fig. 9). The "scanning" can be performed right at the inputs from RPCs, simultaneously on entire planes.

Special, narrow subclass of "non-random 3/4 algorithms" which can be of our interest are:

- **forced 3/4 algorithms** — only **one** of the possible four 3/4 patterns: $(-\phi_2\phi_3\phi_4)$, $(\phi_1 - \phi_3\phi_4)$, $(\phi_1\phi_2 - \phi_4)$, $(\phi_1\phi_2\phi_3-)$, causes a trigger.

Above definitions are summarised in Tab. 1 and illustrated in a pictorial way in Fig. 9.

algorithm	$\phi_1\phi_2\phi_3\phi_4$	$-\phi_2\phi_3\phi_4$	$\phi_1-\phi_3\phi_4$	$\phi_1\phi_2-\phi_4$	$\phi_1\phi_2\phi_3-$
4/4	p	–	–	–	–
strong random 3/4	p_4	p_3	p_3	p_3	p_3
strong non-random 3/4	p_4	p_{31}	p_{32}	p_{33}	p_{34}
weak random 3/4	p	p	p	p	p
weak non-random 3/4	$\max(p_{31}, p_{32}, p_{33}, p_{34})$	p_{31}	p_{32}	p_{33}	p_{34}
forced 3/4, e.g.	p	p	–	–	–

Table 1: Various "3 out of 4" algorithms. Different patterns, which may, in principle, be assigned different p_t, are indicated by different indices of p.

[1] Here we assume that a muon create only one hit per plane. The problem of clusters consisting of several hits in one plane is extensively discussed in [6].

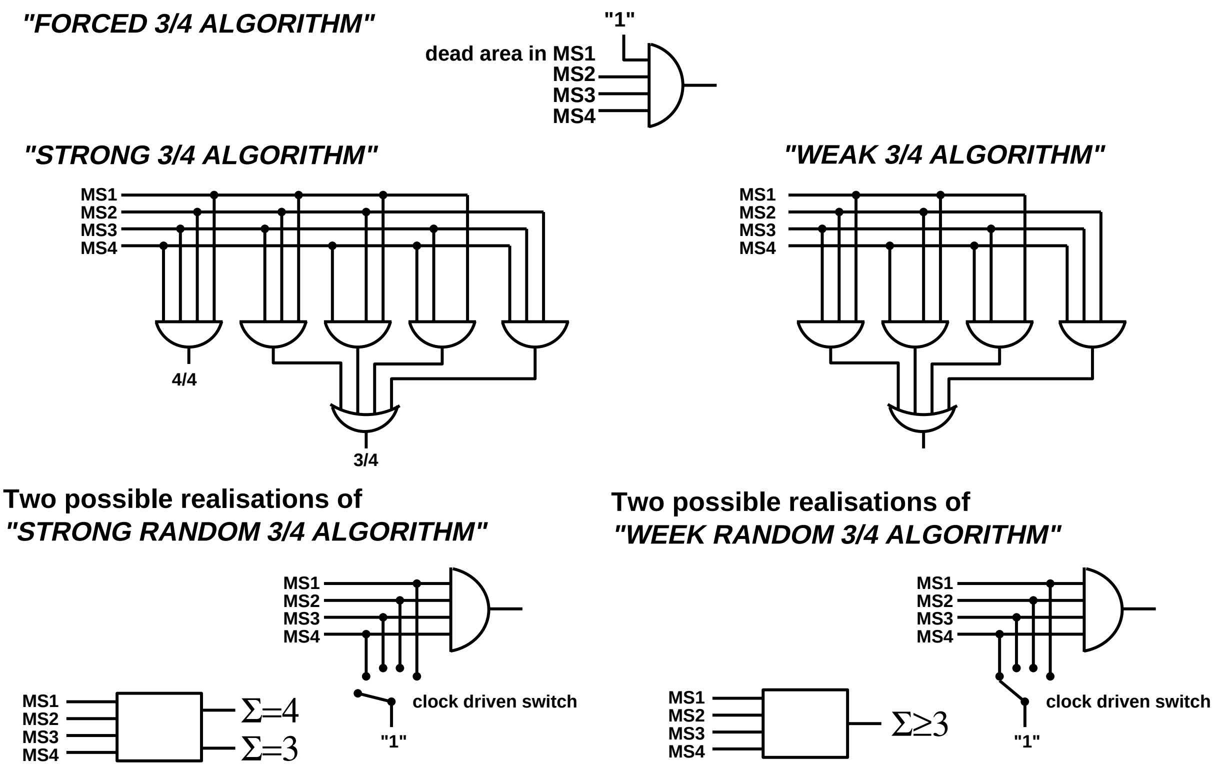

Figure 9: Various "3 out of 4" algorithms.

2.2 Comparison of different algorithms

2.2.1 Forced 3/4 algorithms

Such an algorithm could be useful to correct for dead areas in ϕ. A dead area can be considered as a number of "missing strips" which can be substituted by logical "1" on the processor input (see Fig. 9). This solution, however, cannot be applied to correct for the gaps in Z, between the wheels, because they do not correspond to any set of "missing strips". Therefore, it seems to be necessary to implement some "non-forced" algorithm.

2.2.2 Random and non-random 3/4 algorithms

In principle "non-random" algorithms should give better performance (steeper efficiency curves) than the "random" ones because a "random" algorithm triggers with any 3/4 pattern contained in a 4/4 one, whereas a "non-random" algorithm gives a possibility to choose a particular set of 3/4 patterns, thus being more selective. In practice however the method of selecting valid patterns described in [5, 7] leads to the same sets of patterns in both cases except of low populated tails. Hence, having no strong argument from the performance point of view we choose the "random" algorithms because they are easier to implement.

Additional feature of "random" algorithms is that they do not distinguish between 3/4 caused by a dead space (like e.g. the Z gap) and the RPC intrinsic inefficiency. Thus they automatically correct for this kind of inefficiencies.

2.2.3 Week and strong 3/4 algorithms

The final choice is to be made between the "weak" and the "strong" class. In order to enable a rational choice both algorithms were simulated by the MTRIG program [8] within the GEANT/CMISM framework. The trigger works separately on 39 segments in η (numbered from -19 to 19). In each segment 4 RPC planes are used as shown in Fig. 10.

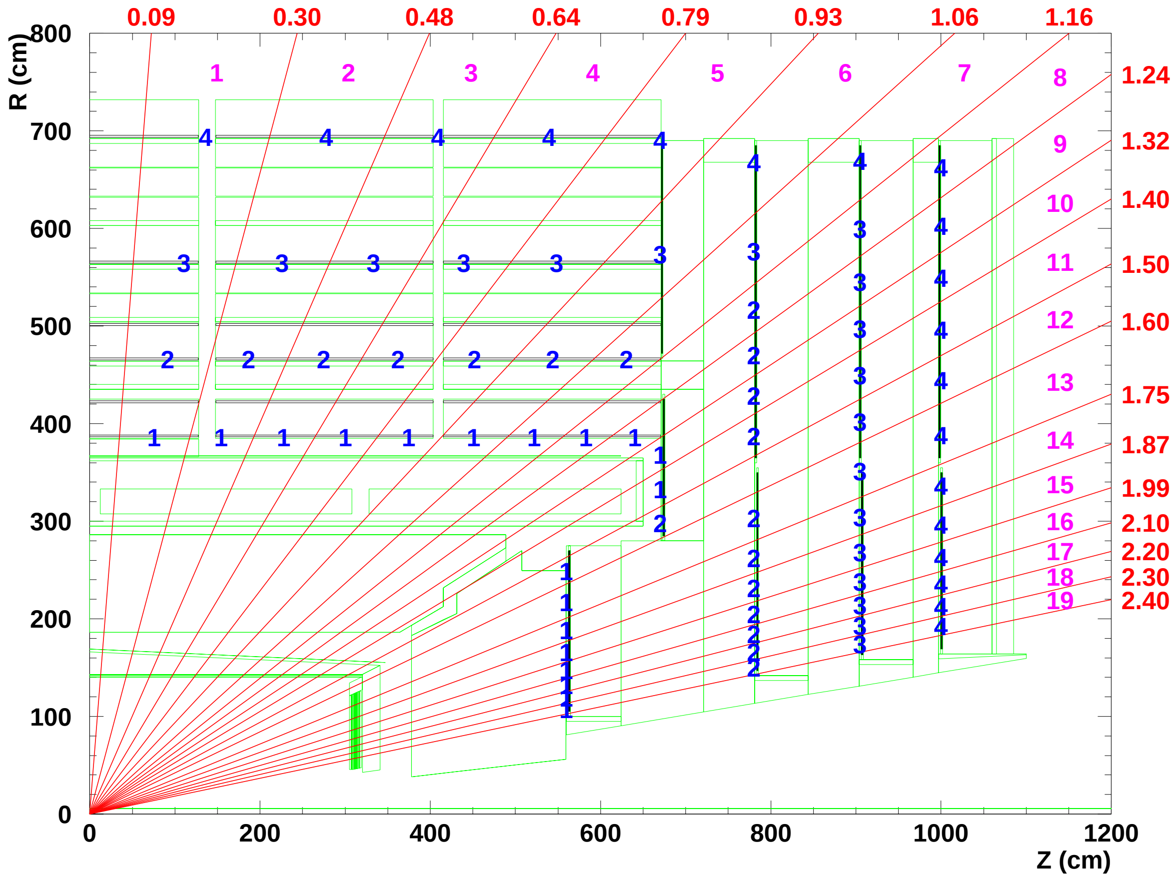

Figure 10: GEANT implementation of the RPC geometry. For each segment its number, η range and 4 planes used for the trigger are marked.

It turns out that the most critical is the transition region between the barrel and the endcap. Geometrical acceptance to record all four or any 3 out of 4 hits is shown in Fig. 11 for five segments of this difficult corner. We can two of them, 0.63-0.79 and 1.16-1.24, consider as "good", because the 4/4 acceptance is about 80% and 90% respectively, and the 3/4 one reaches 100%. The other 3 segments are, however, "bad", because the 4/4 acceptance does not exceed 60% and the 3/4 one is only about 90%. The reson for this in the case of 0.79-0.93 segment is a lack of ϕ-overlap of RPCs in MF1A. In the case of 0.93-1.05 and 1.05-1.16 segments, the loss of efficiency is due to short outer radius of MF2 and MF3 respectively. Originally, this radius was matching the barrel outer radius and equal to 728 cm. Later it was reduced down to 692 cm in order to shorten CSC strips and reduce the overall cost (compare Fig. 1.3 and 7.2 of [1]). In this case, a significant part ($\sim$ 40%) of the fourth triggering plane in this two segments is missing (see Fig. 10), which leads to the observed acceptance losses.

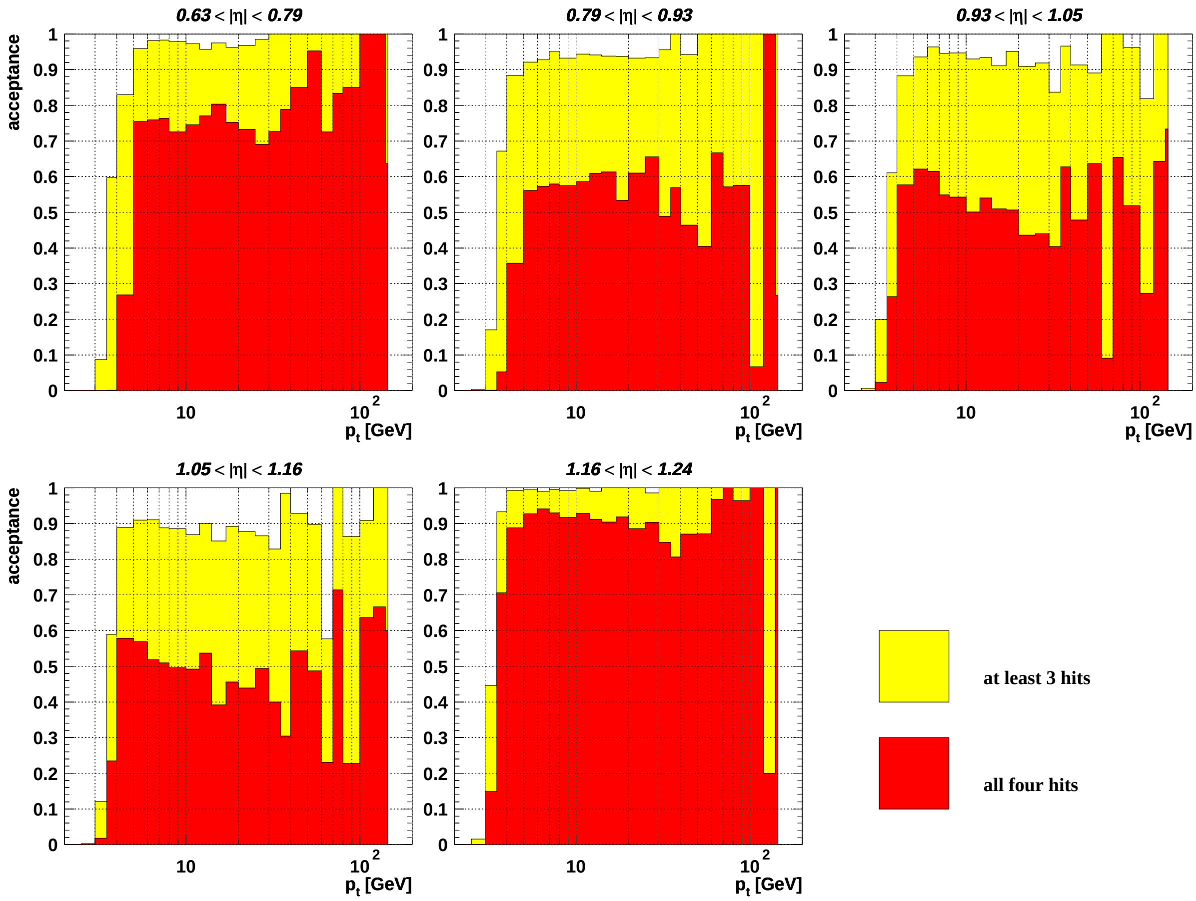

Figure 11: RPC acceptance in several η segments.

Let us now compare the performance of various 3/4 algorithms in one "good" (Fig. 12) and one "bad" (Fig. 13) region. The efficiency curves are plotted in the logarithmic scale to see selectivity of cuts (given by the steepness of the curves), as well as in the expanded linear scale to observe acceptance losses. Let's begin with a "good" region and the 4/4 algorithm. The efficiency curves are rather steep there, but the efficiency is limited to about 80% due to the geometrical acceptance. In contrast, the weak 3/4 algorithm in this region is 100% efficient, but it has very poor momentum selectivity. This is due to the fact that the 4 point measurement of the track curvature is better than the measurements based on only 3 points. When we combine the two algorithms into the strong 3/4 algorithm we combine the good features of both. The resulting efficiency curves are very steep and they reach 100%.

In a "bad" region (Fig. 13), combining the 4/4 algorithm with the weak 3/4 one, we obtain the strong 3/4 algorithm inheriting the bad features of the two. The resulting curves are not very steep and hardly exceed 90%, i.e. the algorithm is neither selective nor efficient. The strong 3/4 algorithm is not worse, however, than the weak 3/4 one.

We can conclude that the strong 3/4 algorithm (random or non-random) is much better than the weak one. Since the random algorithm is easier we are finally going to use the random strong 3/4 one.

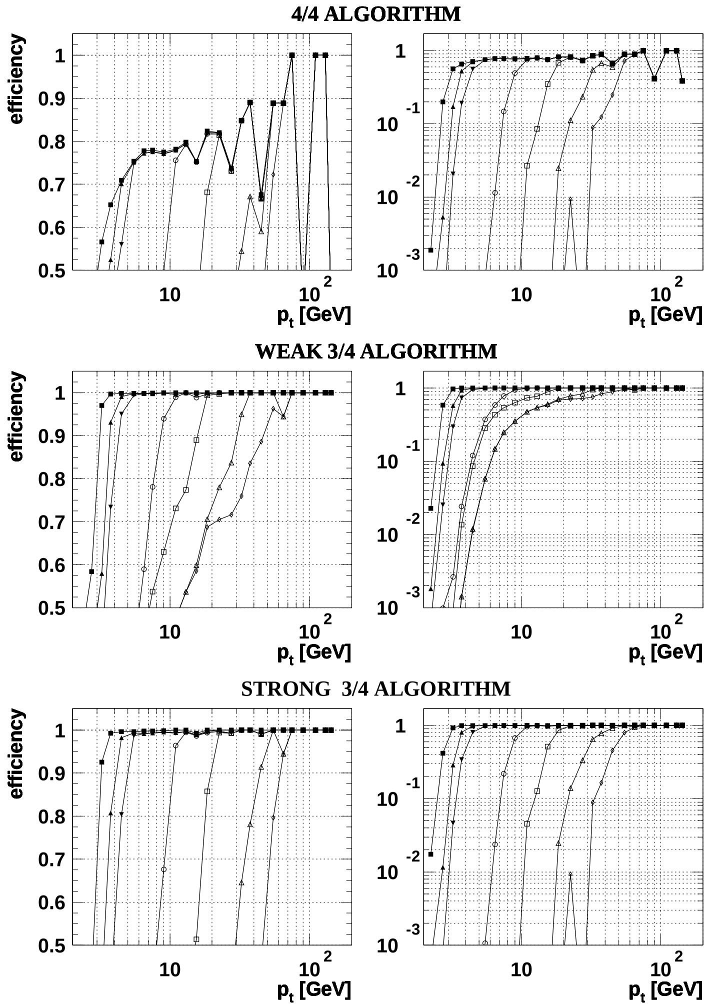

Figure 12: Trigger efficiency at $1.5 < \eta < 1.6$. This is an example of a "good" region, where $P(4/4) > 80\%$ and $P(3/4) \approx 100\%$.

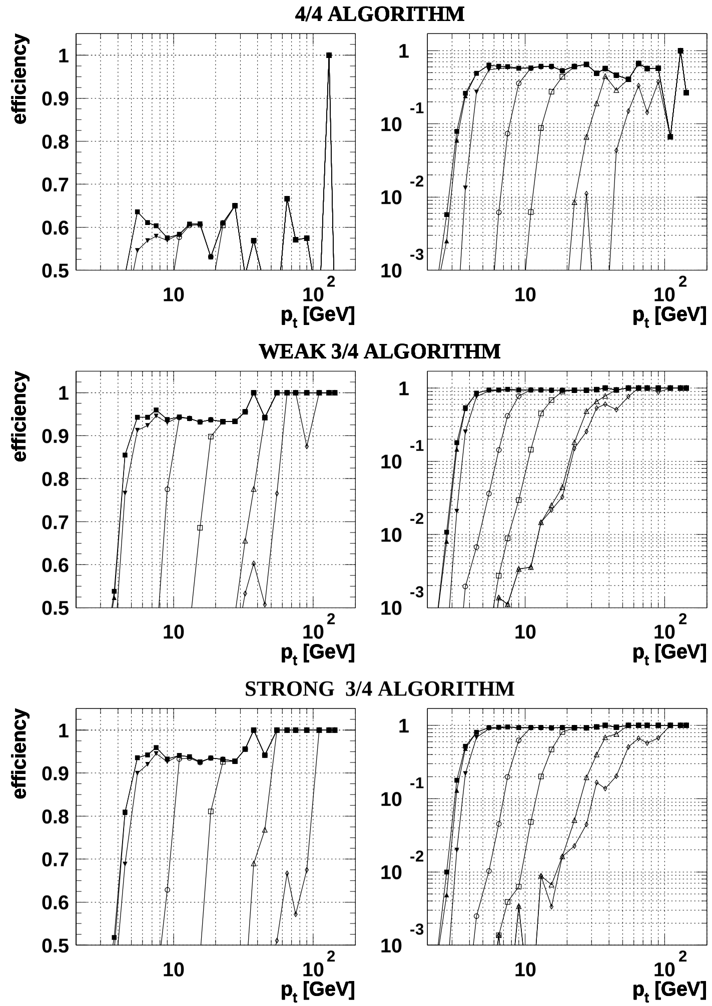

Figure 13: Trigger efficiency at $0.79 < \eta < 0.93$. This is an example of a "bad" region, where $P(4/4) \approx 60\%$ and $P(3/4) \approx 94\%$ mainly due to nonoverlapping structure of MF1A.

3 Requirements for the RPC geometry

From the above study one can also derive the requirements for the RPC geometry. We ought to ensure the 4/4 acceptance of, at least, 80% and 100% in the 3/4 case. This is much stronger requirement than the corresponding one for Cathode Strip Chambers (CSC) or Drift Tubes (DT). This is because the CSC and DT deliver a vector per station, hence coincidence of two stations provides quite precise momentum measurement, and significant background suppression. The RPC chamber delivers only a point, thus coincidence of at least 3 stations is necessary both for momentum estimate and for background reduction.

In order to fulfill the above requirement one needs to design carefully the RPC geometrical layout. As far as possible the following guidelines should be followed:

BARREL

- minimal dead space along the chamber edges
- overlap of gas gaps in Z within each wheel
- overlap of chambers in ϕ at MB4
- maximal use of space in ϕ within the iron at MB1, 2 and 3
- minimal space for the magnet power and cooling chimneys

ENDCAPS

- overlap of chambers in ϕ, also at MF1A and MF1B (it is not the case now [1])
- overlap of gas gaps along R
- outer radius of MF = 728 cm rather than 692 cm (current design), especially at MF2 and MF3.

If possible, the RPC's should be placed at the inner side of the muon stations because eventual showers are less developed there. Moreover, it usually gives better geometrical coverage.

4 Sorting with quality bits

The "strong" algorithm differs from the "weak" one by the fact that it is able to distinguish 3/4 and 4/4 coincidences. Information whether a 3/4 or a 4/4 coincidence occurred should be delivered by a PACT processor as a "quality bit". These bits might be very useful for the global muon trigger combining the RPC and DT/CSC information. They can also effect the sorting algorithm.

- Within the same segment 4/4 should always be chosen in preference to 3/4 irrespectively of the p_t assignment.
- There should be at least one empty segment in η or ϕ between two accepted muons. Separated muons should be sorted according to p_t regardless their quality bits. Therefore the check of the separation can be done either at every sorting step or only at the very end of the sorting tree (e.g. in the global muon trigger). The first solution is more expensive, the second one might be dangerous: multiple copies of a high p_t muon may suppress other, real muons. It should be checked by the simulation whether the fact that the system delivers four muon candidates reduces enough this danger.
- If there are two candidates in the adjacent segments the 4/4 one should be retained and the 3/4 one should be dropped. Consequences of this choice should be checked by simulation.

5 Conclusions

Presented study leads us to the following choices and recommendations:

- RPC trigger will be based on 4 RPC planes. In order to deal with all kind of inefficiencies we have chosen

  strong random 3 out of 4 algorithm

  which takes 4-fold coincidence if there were hits in 4 planes and 3-fold coincidence of any 3 planes in the opposite case.

- This algorithm can work properly only if

  3 out of 4 chambers acceptance = 100%
  4 out of 4 chambers acceptance > 80%

Acknowledgments

Authors would like to acknowledge the support of Polish Committee for Scientific Research under grants KBN-SPUB/P3/201/94 and 115/E-343/SPUB/P03/108/95.

We are very grateful to Pierluigi Zotto for providing the updated muon system geometry in GEANT. We also thank warmly Anna Meneguzzo for crosschecking the results. Finally we would like to express our gratitude to Daniel Denegri and Fabrizio Gasparini for many useful discussions.

References

[1] *The Compact Muon Solenoid – Technical Proposal*, **CERN/LHCC 94-38**, December 1994.

[2] M. Andlinger et al., *Pattern Comparator Trigger (PACT) for the Muon System of the CMS Experiment*, **CMS TN/94-281** and **CERN-PPE/94-227**, submitted to Nucl. Instr. Meth.

[3] IRIS Explorer^{TM} is a trade mark of *Silicon Graphics Inc.*

[4] C. Charlot et al., *CMSIM-CMANA, CMS Simulation Facilities*, **CMS TN/93-63**.

[5] M. Konecki, J. Królikowski, and G. Wrochna, *Simulation study of the single muon, RPC based trigger for CMS*, **CMS TN/92-39**.

[6] M. Górski, M. Konecki, J. Królikowski, I. Kudla and G. Wrochna, *Clusters in RPC and Muon Trigger performance*, **CMS TN/95-107**.

[7] Á. Csilling, M. Konecki, J. Królikowski and G. Wrochna, *Muon Trigger Rates*, **CMS TN/94-282**.

[8] Á. Csilling, M. Konecki, J. Królikowski, G. Wrochna and C. E. Wulz, *Simulation of the CMS Muon Trigger System*, **CMS TN/94-174**.